Table 5. Continued.

rc_AI012807_at	1398765_at	Adaptor-related protein complex 2, mu 1 subunit
S56936_s_at	none	–
S82820mRNA_s_at	none	–
M33747_at	none	–
rc_AI638982_at	none	–
M33746mRNA#2_f_at	none	–
D00362_s_at	none	–
AF044574_at	none	–
S80431_s_at	none	–
rc_AI236284_s_at	none	–
M29249cds_at	none	–
D86745exon_s_at	none	–
X57133mRNA_at	none	–
X74565cds_g_at	none	–
U05784_s_at	none	–
AF087944mRNA_s_at	none	–
X77934cds_at	none	–
rc_AA859519_g_at	none	–
X57999cds_at	none	–
rc_AI231807_g_at	(1367559_at)	–
K01932_f_at	(1367774_at)	–
S72505_f_at	(1367774_at)	–
D00569_at	(1367777_at)	–
D86580_at	(1368376_at)	–
S65555_g_at	(1370030_at)	–

Probe sets whose signals were reported as increased by treatment of glutathione depletors in RG U34A GeneChip analysis were selected from the previous literature, and the corresponding probe sets of RAE 230A GeneChip were determined by referring to "good match probe sets" information provided by Affymetrix. Eighteen probe sets of RG U34A GeneChip did not show any corresponding probe sets in RAE 230A GeneChip, and were presented as "none" in the table. Six probe sets of RG U34A GeneChip had redundant probe sets for the same genes, and the corresponding probe sets are presented in brackets in the table.

was determined by logarithmic conversion of the fold change, where the base was set to 2. The heat map was created using Spotfire software (Spotfire, Inc.). The CYP1A1 mRNA level was determined by referring to signal data measured by 1370269_at gene probe set in GeneChip analysis.

RESULTS

TGP1 score

The TGP1 scores for carcinogenesis-related genes, PPARα-regulated genes and glutathione deficiency-related genes were calculated. For carcinogenesis-related genes, OPZ, CPZ, HCB, SS and WY showed a high TGP1 score among the compounds in the database (Fig. 2 A). For PPARα-regulated genes, WY, CFB, GFZ, BBr and ASA showed high TGP1 score (Fig. 2 B). For glutathione deficiency-related genes, OPZ, BBz, APAP and CMA showed high TGP1 score (Fig. 2 C).

In order to see the dose-dependency of the score, we selected several samples and showed them in Fig. 3A (carcinogenesis-related genes), 3B (PPARα-regulated genes), and 3C (glutathione deficiency-related genes) . It is obvious that the score showed good dose-dependency for all three of the marker gene sets. It is also interesting that some drugs show a sudden and large rise of the score suggesting a threshold of the toxicity at a certain dose level.

Comparison of TGP1 score between rat liver and rat hepatocytes

The TGP1 scores of rat liver and rat hepatocytes were calculated. For carcinogenesis-related genes, the

$$\text{Signal log ratio } (i) = \log_2\left\{ \text{Average Signal } i \text{ (treated)} / \text{Average Signal } i \text{ (control)} \right\}$$

$$\text{Index 1} = \frac{\sum_{i=1}^{N} \text{Signal log ratio } (i)}{\text{Number of probe sets}}$$

$$\text{Index 2} = \frac{\sum_{i=1}^{N} \{\text{Signal log ratio } (i)\}^2}{\text{Number of probe sets}}$$

$$\text{TGP score 1} = (\text{Index 1}) \times (\text{Index 2})$$

Fig. 1. Calculation of TGP1 score.
The signal log ratio was calculated by dividing the mean signal value of the chemical-treated group by that of corresponding control. First, the sum of the signal log ratios for the used probe sets was calculated, and then divided by the number of probe sets used (Index 1). Next, the sum of squared signal log ratios for the used probe sets was calculated, and then divided by the number of probe sets used (Index 2). Finally, the TGP1 score was calculated by multiplying Index 1 with Index 2.

TGP1 scores in rat hepatocyte distributed from -10 to 4, while that of five chemicals, namely OPZ, CPZ, HCB and SS in rat livers showed quite high values exceeding 5 (Fig. 4 A). For PPARα-regulated genes, WY, CFB and BBr showed large TGP1 scores in both rat liver and rat hepatocyte (Fig. 4 B), whereas GFZ and ASA showed large TGP1 scores only in rat liver. For glutathione deficiency-related genes, OPZ, BBz, APAP and CMA showed large TGP1 scores only in rat liver (Fig. 4 C), whereas ANIT, INAH, ET and VPA showed small and negative TGP1 scores only in rat hepatocyte.

Gene expression profile in rat liver and rat hepatocytes

The expression profile of individual genes for carcinogenesis-related gene is shown in Fig. 5. It appears that variations among triplicates (liver *in vivo*) or duplicates (hepatocytes *in vitro*) are relatively small. Although the expression of each marker gene varied among the compounds, trends of gene expression as a whole are represented by the TGP1 scores. As it appeared that the contribution of induction of CYP1A1

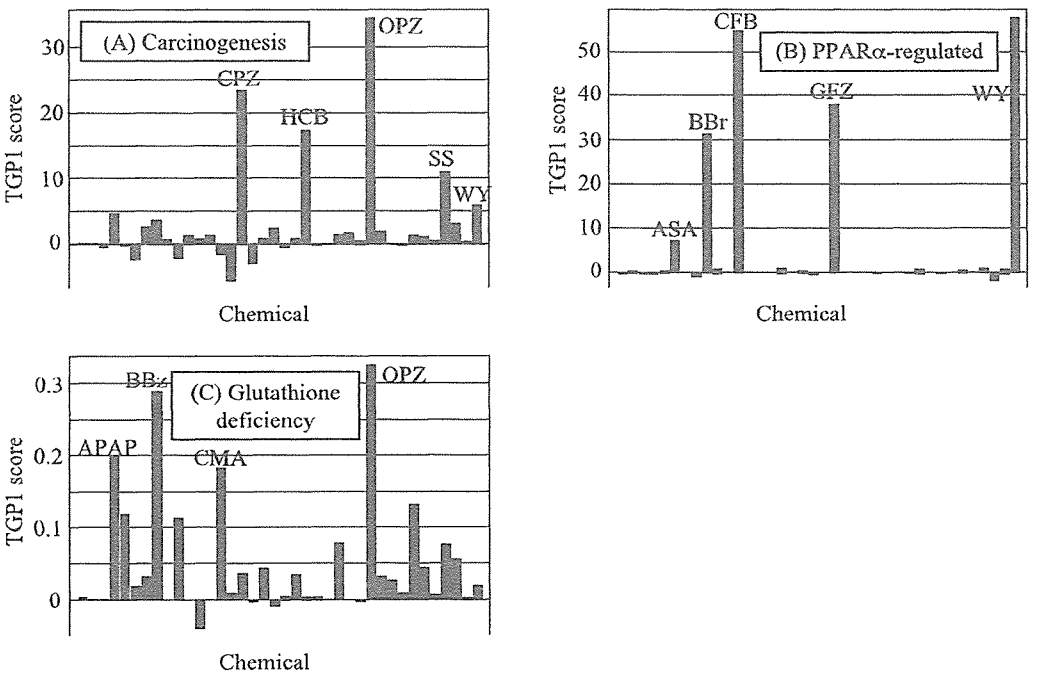

Fig. 2. TGP1 score.
TGP1 scores for (A) carcinogenesis-related genes, (B) PPARα-regulated genes and (C) glutathione deficiency-related genes were calculated for using the TGP database. The data of high dose were used for each chemical. The 38 chemicals are aligned on the abscissa in the order shown in Table 1 and the names are omitted for simplicity. As for the chemicals with high score, their names are indicated by abbreviations in the figure.

mRNA was the largest in the carcinogenesis-related genes, we focused on this gene (Fig. 6). Approximately a 16- to 500-fold increase of CYP1A1 mRNA was observed in OPZ, CPZ, HCB, SS-treated rat livers, whereas that in hepatocytes was only 2- to 8-fold. ANIT and DFNa showed small but consistent changes both *in vivo* and *in vitro*, and APAP and VPA showed no increase (or rather decrease) both *in vivo* and *in vitro*.

Fig. 7 shows the individual expression of glutathione deficiency-related genes *in vivo* and *in vitro*. Again, the variations among triplicates (liver *in vivo*) or duplicates (hepatocytes *in vitro*) appeared to be small, and the trends of gene expression as a whole were well represented by the TGP1 scores.

DISCUSSION

The objective of this study was to establish a one-dimensional score, which reflects the level of gene expression changes in certain biomarker gene sets. Such a score would be useful particularly when a large-scale toxicogenomics database and multiple biomarker information are available simultaneously. In the present study, we examined the usefulness of the score, named as TGP1, based on the signal log ratio values of the chemical-treated to the vehicle-treated rats.

As shown in Fig. 1, the TGP1 score comprised two elements, Index 1 and Index 2. Index 1 was set to capture the general tendency of gene expression changes; the absolute value would be high when the direction of the change is concomitant, whereas it would be low when they are random. In the present study, we selected three biomarker gene sets in which their expression is supposed to be uniformly up-regulated by treatment. The next element, Index 2, was set to capture the general size of gene expression changes, not considering their change in direction toward up- or

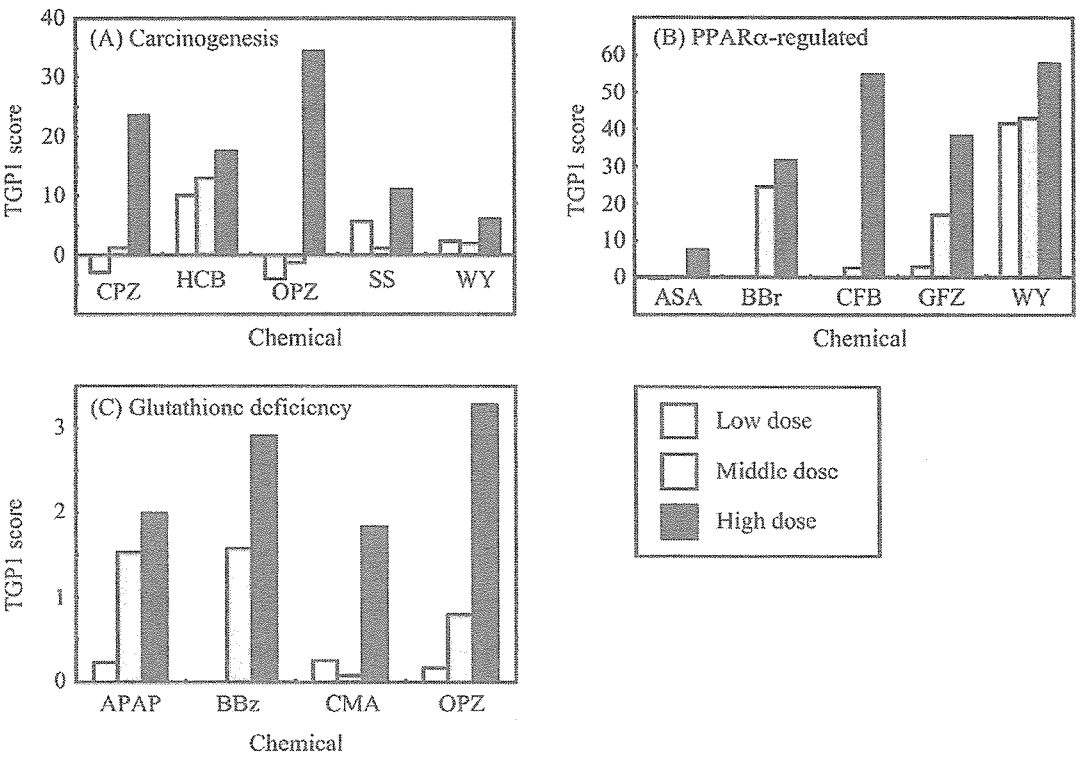

Fig. 3. Dose-dependency of TGP1 score.
The chemicals showing high TGP1 score (indicated in Figure 2) at high dose were selected and TGP1 scores for (A) carcinogenesis-related genes, (B) PPARα-regulated genes and (C) glutathione deficiency-related genes were calculated for low and middle doses in order to show dose-dependency. The abbreviations of the chemicals are shown in Table 1.

down-regulation by the chemical treatments. Since Index 2 includes the square of the signal log ratio, it tends to be higher when a biomarker gene set includes genes that show large changes in their mRNA levels. To examine the usefulness of the TGP1 score, three biomarker gene sets were selected from the previous literature whose expression levels are up-regulated by carcinogens (Table 3), PPARα activators (Table 4) and glutathione depletors (Table 5).

For carcinogenesis-related genes, the TGP1 score was high in rats treated with OPZ, CPZ, HCB, SS and WY (Fig. 2 A). OPZ is reported to have weak genotoxicity (Martelli *et al.*, 1998). CPZ and WY are reported to be non-genotoxic carcinogens in rodent (Gocke, 1996; Peters *et al.*, 1997). HCB and SS are reported to have carcinogenic potential in rodents (Smith *et al.*, 1985; Iatropoulos *et al.*, 1997). Thus, the TGP1 score appears to well express the carcinogenic risk of the chemicals. For PPARα-regulated genes, the TGP1 score was high in rats treated with CFB, WY, GFZ, BBr and ASA (Fig. 2 B). Of these, CFB, WY and GFZ are known to be potent PPARα activators (Gonzalez *et al.*, 1998). Besides these direct PPARα activators, it was reported that BBr has peroxisome proliferator activity (Bichet *et al.*, 1990). In addition, several non-steroidal anti-inflammatory drugs are reported to activate PPARα (Lehmann *et al.*, 1997), and therefore a high TGP1 score observed in ASA-treated rat liver would be reasonable. These results indicate that the TGP1 score works to express the PPARα-modulating property of the chemicals. For glutathione deficiency-related genes, the TGP1 score was high in rats treated with OPZ, BBz, APAP and CMA (Fig. 2 C). Of these, BBz, APAP and CMA are reported to deplete the hepatic glutathione content when overdosed (Lake *et al.*, 1989; Szymanska, 1996; James *et al.*, 2003). Although OPZ has not been reported to deplete hepatic glutathione in rats, it could be highly possible at extremely high dose, since OPZ attacks SH of gastric proton pump at low pH and this effect is prevented by

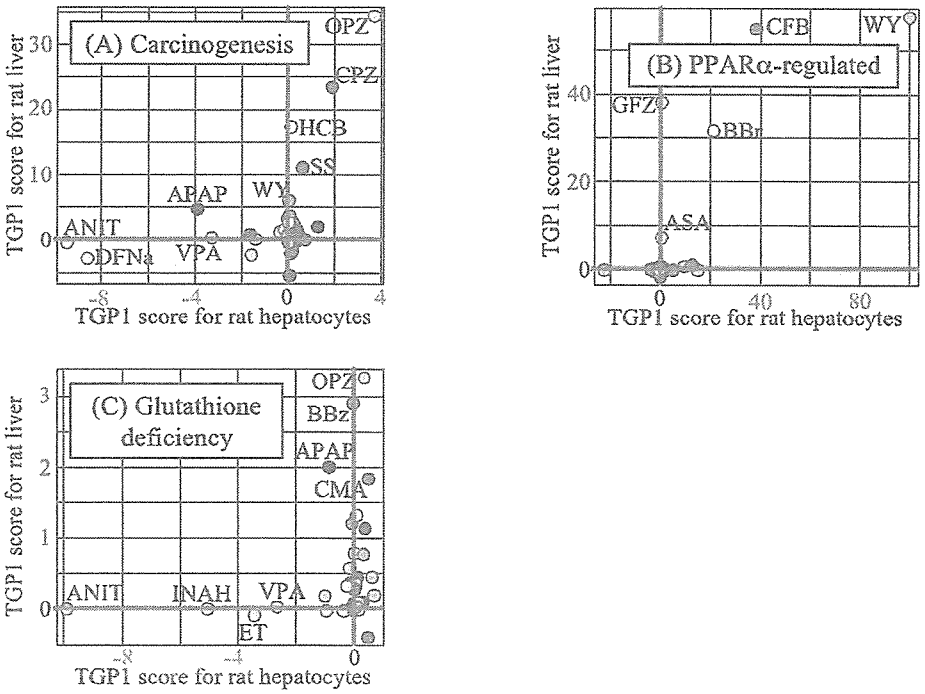

Fig. 4. Comparison of TGP1 scores between rat liver and rat hepatocytes.
Scatter plots of TGP1 scores for rat liver and rat hepatocytes are presented using (A) carcinogenesis-related genes, (B) PPARα-regulated genes and (C) glutathione deficiency-related genes.

glutathione (Morii *et al.*, 1989), and OPZ-glutathione conjugates are found in rat serum as metabolites (Weidolf *et al.*, 1992). Nonetheless, the results obtained from the three biomarker gene sets demonstrated that the TGP1 score successfully captured the characteristics of the compounds stored in our database.

In the next step, we compared the TGP1 scores between rat liver and hepatocytes. Since the TGP1 score is a one-dimensional value, we can make the comparison by plotting on X-Y coordinates. For carcinogenesis-related genes, TGP1 scores for some compounds including OPZ and CPZ showed positive correlation between rat liver and rat hepatocytes (Fig. 4 A). However, absolute values of TGP1 scores for hepatocytes were much smaller than those for liver, indicating that the genes included in the gene sets did not respond in the same way to the compounds between *in vivo* and *in vitro*. Similarly, the TGP1 score for glutathione deficiency-related genes did not show any correlation between liver and hepatocytes (Fig. 4 C), indicating that these gene sets can only be applied to data analysis of rat liver, and not to rat hepatocytes. ForPPARα-regulated genes, however, the scores for WY, CFB and BBr showed good positive correlation between rat liver and rat hepatocytes (Fig. 4 B). In contrast to the case of carcinogenesis-related genes, the absolute values of TGP1 scores were similar for *in vivo* and *in vitro*. It seems these gene sets could be used for assessing PPARα-modulating effects of chemicals in rat liver by using rat hepatocytes as an alternative experimental system. One of the premises of toxicogenomics research is to scale down toxicity studies from *in vivo* to an *in vitro* system, thereby reducing the number of experimental animals and the amount of test substances used (Boess *et al.*, 2003). It is expected that the TGP1 score enables us to suggest certain toxicological endpoints *in vivo*, which can be evaluated by *in vitro* systems using a large-scale toxicogenomics database and specific biomarker gene sets, such as PPARα-reg-

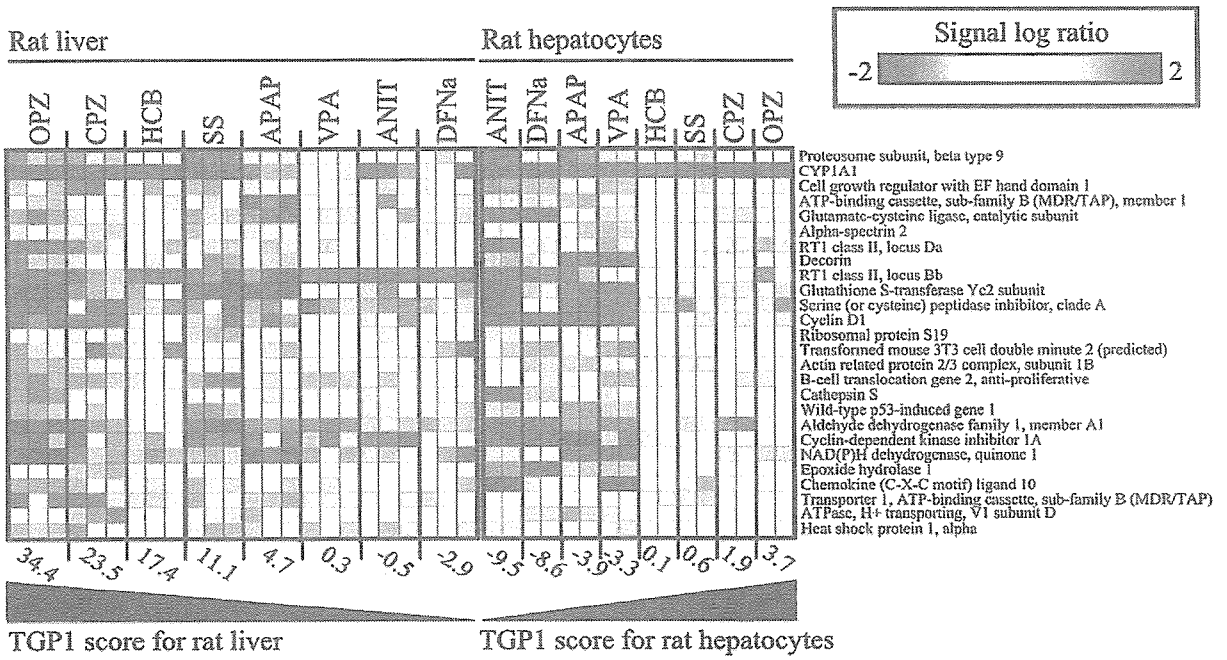

Fig. 5. Gene expression profile of carcinogenesis-related genes.
The fold change value for each of the carcinogenesis-related genes was calculated by dividing the signal value of chemical-treated rats or rat hepatocytes by the mean signal value of corresponding vehicle-treated rats (n=3) or rat hepatocytes (n=2), respectively, and the fold change values were converted to logarithm values where the base was set to 2. The heat map representing individual expression levels of carcinogenesis-related genes was created using the logarithm values of fold changes.

ulated genes.

The TGP1 score is useful for quickly surveying the gene expression changes in biomarker gene sets for multiple samples. However, the significance of changes in gene expression should be investigated in detail for the next step of data analysis. In the present study, the compounds whose TGP1 scores were relatively high or low in either rat liver or rat hepatocytes were selected, and expression profiles of carcinogenesis-related genes and glutathione deficiency-related genes are presented in Fig. 5 and Fig. 7, respectively. For carcinogenesis-related gene sets, CYP1A1 appeared to be the most remarkable gene that strongly affects the TGP1 score. The importance of the CYP1A1 gene in TGP1 score calculation for carcinogenesis-related gene sets is evident in Fig. 6 as well. CYP1A1 is under control of arylhydrocarbon receptor, a transcription factor that has been reported to play a key role in liver tumor promotion (Bock and Kohle, 2005). Therefore, the biological significance suggested by a high TGP1 score using carcinogenesis-related genes was thought to be appropriate for evaluating the carcinogenic risk of chemicals. On the other hand, genes that strongly affect the TGP1 score for glutathione deficiency-related genes were found to be aldo-keto reductase family 7, glutathione S-transferase Yc2 subunit, metallothionein or NAD(P)H dehydrogenase (Fig. 7). It is crucial to determine and investigate such key genes that strongly affect the TGP1 score to elucidate the molecular mechanism of toxicity.

One of the most promising goals of toxicogenomics application in drug development is an improved quality of safety assessment in human cases from experimental animal data, and the TGP database is constructed to achieve this goal by collecting both rat and human microarray data. When inter-species data analysis is challenged, however, a probe set conversion process from rat to human-like ortholog conversion is required. However, such converted-probe sets usually contain low-quality data for measuring gene expression signal in human samples. In such cases, straightforward data analysis would lead to the wrong conclusion. Therefore, the TGP1 score is thought to be inadequate to compare samples across the species. Additional scores that overcome this drawback should be needed for efficient data analysis of large-scale microarray database such as our TGP database.

In conclusion, we tested a simple one-dimensional score, named as TGP1, that reflects the level of gene expression changes in certain biomarker gene sets. The usefulness of this score was demonstrated using the TGP database. The score is useful for surveying the expression changes in multiple biomarker gene sets using the large-scale toxicogenomics database, which can reduce the labor- and time-consuming task of conventional multivariate statistical analysis. This scoring system is now incorporated in our analysis system where TGP1 scores are automatically calculated and displayed. Additional sophisticated one-dimensional scores should be invented to facilitate gene expression analysis for a large-scale toxicogenomics database with multiple biomarker gene sets.

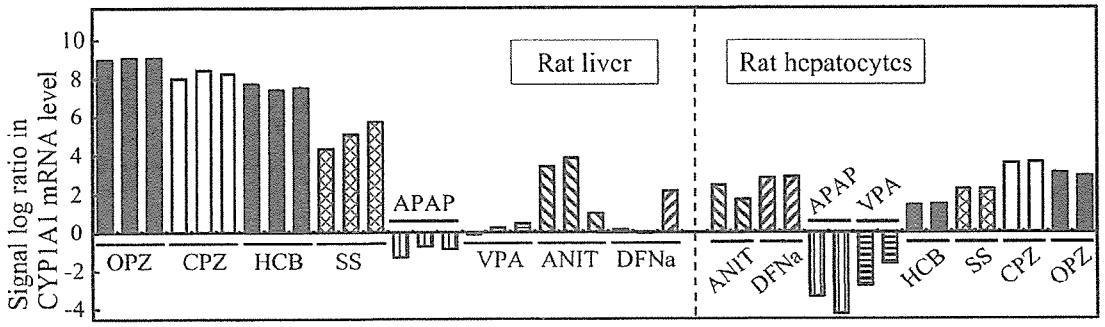

Fig. 6. Change in CYP1A1 mRNA level.
The fold change value for the CYP1A1 gene determined by 1370269_at probe set in GeneChip analysis was calculated by dividing the signal value of chemical-treated rats or rat hepatocytes by the mean signal value of corresponding vehicle-treated rats (n=3) or rat hepatocytes (n=2), respectively, and the fold change values were converted to logarithm values where the base was set to 2.

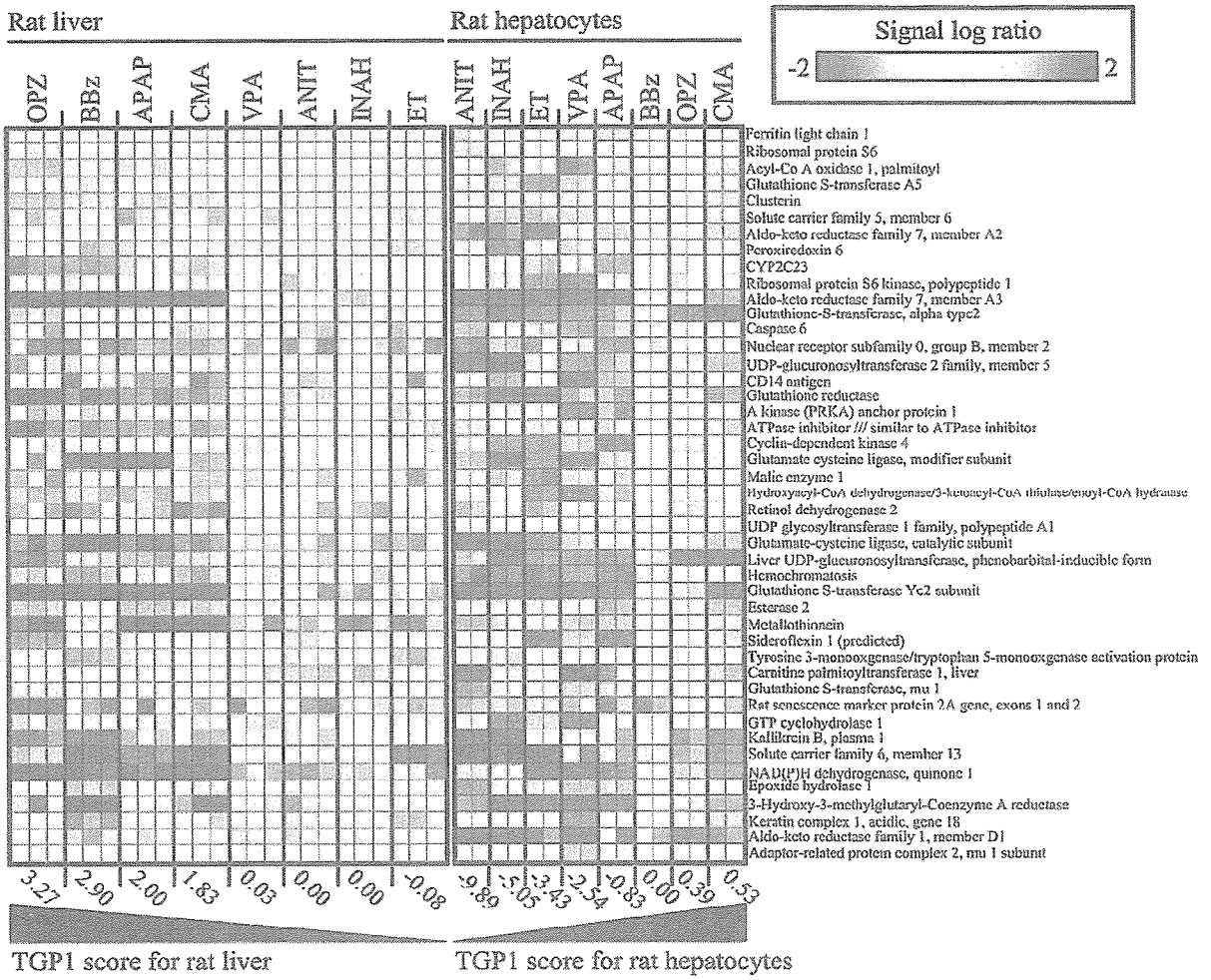

Fig. 7. Gene expression profile of glutathione deficiency-related genes.
The fold change value for each of the glutathione deficiency-related genes was calculated by dividing the signal value of chemical-treated rats or rat hepatocytes by the mean signal value of corresponding vehicle-treated rats (n=3) or rat hepatocytes (n=2), respectively, and the fold change values were converted to logarithm values where the base was set to 2. The heat map representing individual expression levels of glutathione deficiency-related genes was created using the logarithm values of fold changes.

ACKNOWLEDGMENT

This study was supported in part by a grant from the Ministry of Health, Labor and Welfare (H14-Tox-ico-001).

REFERENCES

Bichet, N., Cahard, D., Fabre, G., Remandet, B., Gouy, D. and Cano, J.P. (1990): Toxicological studies on a benzofuran derivative. III. Comparison of peroxisome proliferation in rat and human hepatocytes in primary culture. Toxicol. Appl. Pharmacol., **106**, 509-517.

Bock, K.W. and Kohle, C. (2005): Ah receptor- and TCDD-mediated liver tumor promotion: clonal selection and expansion of cells evading growth arrest and apoptosis. Biochem. Pharmacol., **69**, 1403-1408.

Boess, F., Kamber, M., Romer, S., Gasser, R., Muller, D., Albertini, S. and Suter, L. (2003): Gene expression in two hepatic cell lines, cultured primary hepatocytes, and liver slices compared to the *in vivo* liver gene expression in rats: Possible implications for toxicogenomics use of *in vitro* systems. Toxicol. Sci., **73**, 386-402.

Boverhof, D.R. and Zacharewski, T.R. (2006): Toxicogenomics in risk assessment: Applications and needs. Toxicol. Sci., **89**, 352-360.

Draghici, S. (2003): Analysis and visualization tools. In Data Analysis Tools for DNA Microarrays (Etheridge, A.M., Gross, L.J., Lenhart, S., Maini, P. K., Safer, H. M. and Voit, E. O., eds.), pp. 231-261. CRC Press, London.

Ellinger-Ziegelbauer, H., Stuart, B., Wahle, B., Bomann, W. and Ahr, H.J. (2004): Characteristic expression profiles induced by genotoxic carcinogens in rat liver. Toxicol. Sci., **77**, 19-34.

Gocke, E. (1996): Review of the genotoxic properties of chlorpromazine and related phenothiazines. Mutat. Res., **366**, 9-21.

Gonzalez, F.J., Peters, J.M. and Cattley, R.C. (1998): Mechanism of action of the nongenotoxic peroxisome proliferators: Role of the peroxisome proliferator-activator receptor alpha. J. Natl. Cancer Inst., **90**, 1702-1709.

Iatropoulos, M.J., Williams, G.M., Abdo, K.M., Kari, F.W. and Hart, R.W. (1997): Mechanistic studies on genotoxicity and carcinogenicity of salicylazosulfapyridine an anti-inflammatory medicine. Exp. Toxicol. Pathol., **49**, 15-28.

Ito, K., Kiyosawa, N., Kumagai, K., Manabe, S., Matsunuma, N. and Yamoto, T. (2006): Molecular mechanism investigation of cycloheximide-induced hepatocyte apoptosis in rat livers by morphological and microarray analysis. Toxicology, **219**, 175-186.

James, L.P., Mayeux, P.R. and Hinson, J.A. (2003): Acetaminophen-induced hepatotoxicity. Drug Metab. Dispos., **31**, 1499-1506.

Kaminski, N. and Friedman, N. (2002): Practical approaches to analyzing results of microarray experiments. Am. J. Respir. Cell Mol. Biol., **27**, 125-132.

Kiyosawa, N., Ito, K., Sakuma, K., Niino, N., Kanbori, M., Yamoto, T., Manabe, S. and Matsunuma, N. (2004a): Evaluation of glutathione deficiency in rat livers by microarray analysis. Biochem. Pharmacol., **68**, 1465-1475.

Kiyosawa, N., Tanaka, K., Hirao, J., Ito, K., Niino, N., Sakuma, K., Kanbori, M., Yamoto, T., Manabe, S. and Matsunuma, N. (2004b): Molecular mechanism investigation of phenobarbital-induced serum cholesterol elevation in rat livers by microarray analysis. Arch. Toxicol., **78**, 435-442.

Lake, B.G., Gray, T. J., Evans, J.G., Lewis, D.F., Beamand, J.A. and Hue, K.L. (1989): Studies on the mechanism of coumarin-induced toxicity in rat hepatocytes: Comparison with dihydrocoumarin and other coumarin metabolites. Toxicol. Appl. Pharmacol., **97**, 311-323.

Lehmann, J.M., Lenhard, J.M., Oliver, B.B., Ringold, G.M. and Kliewer, S.A. (1997): Peroxisome proliferator-activated receptors alpha and gamma are activated by indomethacin and other non-steroidal anti-inflammatory drugs. J. Biol. Chem., **272**, 3406-3410.

Liu, G., Loraine, A.E., Shigeta, R., Cline, M., Cheng, J., Valmeekam, V., Sun, S., Kulp, D. and Siani-Rose, M.A. (2003): NetAffx: Affymetrix probesets and annotations. Nucleic Acids Res., **31**, 82-86.

Martelli, A., Mattioli, F., Mereto, E., Brambilla Campart, G., Sini, D., Bergamaschi, G. and Brambilla, G. (1998): Evaluation of omeprazole genotoxicity in a battery of *in vitro* and *in vivo* assays. Toxicology, **130**, 29-41.

Morii, M., Takata, H. and Takeguchi, N. (1989): Acid activation of omeprazole in isolated gastric vesicles, oxyntic cells, and gastric glands. Gastroenterol., **96**, 1453-1461.

Peters, J.M., Cattley, R.C. and Gonzalez, F.J. (1997): Role of PPAR alpha in the mechanism of action of the nongenotoxic carcinogen and peroxisome proliferator Wy-14,643. Carcinogenesis, **18**, 2029-2033.

Richert, L., Lamboley, C., Viollon-Abadie, C., Grass, P., Hartmann, N., Laurent, S., Heyd, B., Mantion, G., Chibout, S.D. and Staedtler, F. (2003): Effects of clofibric acid on mRNA expression profiles in primary cultures of rat, mouse and human hepatocytes. Toxicol. Appl. Pharmacol., **191**, 130-146.

Sawada, H., Takami, K. and Asahi, S. (2005): A toxicogenomic approach to drug-Induced phospho-

lipidosis: Analysis of its induction mechanism and establishment of a novel *in vitro* screening system. Toxicol. Sci., **83**, 282-292.

Sehata, S., Kiyosawa, N., Makino, T., Atsumi, F., Ito, K., Yamoto, T., Teranishi, M., Baba, Y., Uetsuka, K., Nakayama, H. and Doi, K. (2004): Morphological and microarray analysis of T-2 toxin-induced rat fetal brain lesion. Food Chem. Toxicol., **42**, 1727-1736.

Smith, A.G., Francis, J.E., Dinsdale, D., Manson, M.M. and Cabral, J.R. (1985): Hepatocarcinogenicity of hexachlorobenzene in rats and the sex difference in hepatic iron status and development of porphyria. Carcinogenesis, **6**, 631-636.

Szymanska, J.A. (1996): Biochemical alterations as measures of acute and subacute hepatotoxicity of 1,3-dibromobenzene in rat. Arch. Toxicol., **71**, 99-106.

Takashima, K., Mizukawa, Y., Morishita, K., Okuyama, M., Kasahara, T., Toritsuka, N., Miyagishima, T., Nagao, T. and Urushidani, T. (2006): Effect of the difference in vehicles on gene expression in the rat liver-analysis of the control data in the Toxicogenomics Project Database. Life Sci., **78**, 2787-2796.

Urushidani, T. and Nagao, T. (2005): Toxicogenomics: The Japanese initiative. In Handbook of Toxicogenomics - Strategies and Applications (Borlak, J., ed.), pp. 623-631. Wiley - VCH.

Weidolf, L., Karlsson, K.E. and Nilsson, I. (1992): A metabolic route of omeprazole involving conjugation with glutathione identified in the rat. Drug Metab. Dispos., **20**, 262-267.

The Journal of Toxicological Sciences,
Vol.31, No.5, 449-469, 2006

COMPARISON OF GENE EXPRESSION PROFILES AMONG PAPILLA, MEDULLA AND CORTEX IN RAT KIDNEY

Kotaro TAMURA[1], Atsushi ONO[1], Toshikazu MIYAGISHIMA[1], Taku NAGAO[2] and Tetsuro URUSHIDANI[1,3]

[1]*Toxicogenomics Project, National Institute of Biomedical Innovation, 7-6-8 Saito-Asagi, Ibaraki, Osaka 567-0085, Japan*

[2]*National Institute of Health Sciences, 1-18-1 Kamiyoga, Setagaya-Ku, Tokyo 158-8501, Japan*

[3]*Department of Pathophysiology, Faculty of Pharmaceutical Sciences, Doshisha Women's College of Liberal Arts, Kodo, Kyotanabe, Kyoto 610-0395, Japan*

(Received August 18, 2006; Accepted September 11, 2006)

ABSTRACT — The aim of this study was to compare gene expression profiles in the different kidney regions as the basis for toxicogenomics. Rat kidney was separated into papilla, medulla and cortex, and total RNA was isolated from these and from the whole slice. Gene expression profiling was performed using Affymetrix Rat Genome 230 2.0 Array. When global normalization was applied, the expression of β-actin or GAPDH varied among the regions. It was considered that such a comparison could not be made, especially between papilla and other portions, since the production of total mRNA in the former was relatively low. In fact, ANOVA was performed on the gene expression values with global normalization in papilla, medulla, cortex, and whole slice, and the numbers of genes appeared to be the highest in papilla. It was also observed that many genes showed their maximum or minimum in the whole slice, which was theoretically impossible. To overcome the problems associated with global normalization, the "percelome" normalization (a way to obtain the values directly related to the copies of mRNA per cell) was employed to compare the regions. In applying this procedure, probe sets with regional difference in expression were efficiently extracted by ANOVA. When they were sorted by the fold difference to other regions, the higher rank was occupied by genes characteristic of the functions of kidney, i.e., channels, transporters and metabolic enzymes. Some of them were consistent with the literature and were related to pathophysiological phenomena. Comprehensive comparison of data of gene expression in the renal anatomical area will greatly enhance studies of the physiological function and mechanism of toxicity in kidney.

KEY WORDS: Toxicogenomics, Kidney, Gene expression, Regional difference, Rat

INTRODUCTION

The Toxicogenomics Project is a 5-year collaborative project by the National Institute of Health Sciences (NIHS) and 17 pharmaceutical companies in Japan which was started in 2002 (Urushidani and Nagao, 2005). In April 2005, some rearrangements were made and now the project is conducted by NIHS, the National Institute of Biomedical Innovation, and 15 pharmaceutical companies. Its aim is to construct a large-scale toxicology database of transcriptome for prediction of toxicity of new chemical entities in the early stage of drug development. About 150 chemicals, mainly medicinal compounds, have been selected, and the following are examined for each. The *in vivo* test using rat consists of a single administration test (3, 6, 9 and 24 hr with 4 dose levels including vehicle control) as well as a repeated administration test (3, 7, 14 and 28 days with 4 dose levels including vehicle control), and then data of body weight, general symptoms, histopathological examination of liver and kidney, and blood biochemistry are obtained from each animal. Gene

Correspondence: Tetsuro URUSHIDANI (E-mail: turushid@dwc.doshisha.ac.jp)

expression in liver (and kidney in some cases) is comprehensively analyzed by using Affymetrix GeneChip. An *in vitro* test using rat and human hepatocytes is also carried out to accomplish the bridging between the species. Although the main target of the project is liver, about 10 of the chemicals are typical nephrotoxicants and many others exhibited nephrotoxicity in addition to hepatotoxicity. In our project, we plan to perform gene expression analysis of kidney for up to 30 such chemicals.

Although the toxicogenomics technique is established as a powerful tool for prediction of nephrotoxicity of drugs (Thukra *et al.*, 2005), it is well known that kidney consists of a variety of cell types and that the physiological functions, including gene expression, differ between the anatomical portions, i.e., papilla, medulla, and cortex. Therefore, we expected that different gene expression profiles would be obtained either when kidney is analyzed as a whole or separated into each portion. For an exploratory test, we checked potential region-related differences in gene expression before starting analysis of drug effects on the kidney.

In employing global normalization, based on the assumption that the total amount of mRNA is constant, it can cause a bias in the comparison of the different portions, since the rate of transcription varies with the cell types. In our project, gene expression values can be converted to a value proportional to the copies of mRNA per cell (the values normalized by externally adding standard mRNA in an amount proportional to the DNA content in the homogenate) by employing a system, "percellome" (Kanno *et al.*, 2006). In the present study, quantification by this system was compared to that of global normalization.

MATERIALS AND METHODS

Animals and Sampling

Male Sprague-Dawley rats were purchased from Charles River Japan Inc., (Kanagawa, Japan) at 5-weeks of age. After a 7-day quarantine and acclimatization period, 6 of the animals were euthanized by exsanguination from the abdominal veins and arteries under ether anesthesia. Kidneys were collected from each animal, and sliced horizontally at its middle portion with ca. 1 mm thickness by a pair of razor blades with a spacer in between. The slice was put into RNA later (Ambion, Austin, TX, USA) overnight for expression profiling. The fixed slices from three (No. 1 to 3) out of 6 animals were then separated into papilla, medulla, and cortex, as shown in Fig. 1. The remaining three (No. 4 to 6) were analyzed as a whole slice. The experimental protocols were reviewed and approved by the Ethics Review Committee for Animal Experimentation of the National Institute of Health Sciences.

Expression profiling

The kidney samples (whole slice, papilla, medulla and cortex) were homogenized using Mill Mixer (Qiagen) and zirconium beads. Total RNA was isolated from the kidney homogenate using RNeasy kit. Purity of the RNA was checked by gel electrophoresis, and the 260/280 nm ratio was between 2.0-2.2. Microarray analysis was conducted on 3 samples for each group by using GeneChip Rat Genome 230

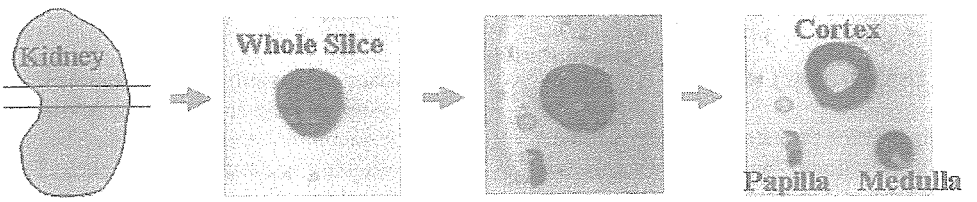

Animal No. 1 ⇒ Whole slice No. 1
Animal No. 2 ⇒ Whole slice No. 2
Animal No. 3 ⇒ Whole slice No. 3
Animal No. 4 ⇒ Papilla No. 4, Medulla No. 4, Cortex No. 4
Animal No. 5 ⇒ Papilla No. 5, Medulla No. 5, Cortex No. 5
Animal No. 6 ⇒ Papilla No. 6, Medulla No. 6, Cortex No. 6

Fig. 1. Sampling and preparation of kidney for GeneChip analysis.

2.0 Arrays (Affymetrix, Santa Clara, CA, USA) containing 31,099 probe sets. The procedure was basically conducted according to the manufacturer's instructions using Superscript Choice System (Invitrogen, Carlsbad, CA, USA) and T7-(dT)24-oligonucleotide primer (Affymetrix) for cDNA synthesis, cDNA Cleanup Module (Affymetrix) for purification, and IVT Labeling Kit (Affymetrix) for synthesis of biotin-labeled cRNA. Twenty μg of the fragmented cRNA was hybridized to a Rat Genome 230 2.0 Array for 18 hr at 45°C at 60 rpm after which the array was washed and stained by streptavidin- phycoerythrin using Fluidics Station 450 (Affymetrix) and then scanned by Gene Array Scanner (Affymetrix).

Percellome normalization

We primarily use global mean normalization for data analysis in our project. However, to compare a sample from a different kidney region, in which the activity of transcription might be different, global normalization based on the total mRNA appeared not to provide the correct result. In the present study, we employed "percellome normalization" to normalize data as well.

The Percellome method reported by Kanno *et al.* (2006) was shown to be effective to compare the data from different tissues or different platform. In this method, the grade-dosed spike cocktail (GSC), which consists of five different Bacillus subtilis mRNA with different concentrations, was added to the tissue homogenate in proportion to its DNA contents before RNA extraction, assuming that all the cells contain a fixed amount of genomic DNA (g/cell) across the samples. The copy number of the RNA in one cell was calculated from the function of signal values of GSC and their copy number. Therefore, the effect of the difference in the total gene expression between samples can be avoided and a direct comparison of the expression data of samples from different sources is enabled.

The GSC used in this study was generously provided by Dr. Kanno, and the experimental procedure and calculations of the percellome method was conducted according to the original procedure. By separate experiments, we confirmed that GSC did not affect signals of other RNA and that the effect on global mean value was negligible.

Statistical Analysis

The data was analyzed by using GeneSpring version 6.1 (Silicon Genetics, Santa Clara, CA, USA), 2003 (Microsoft, Redmond, WA, USA) and MeV version 3.1 (The Institute for Genomic Research, Rockville, MD, USA). Expression data were customarily normalized using the mean value, multiplied by 500 (global mean normalization). Filtering of the data was performed either by flags (present, absent and marginal call) or ANOVA (Snedecor and Cochran, 1989).

RESULTS

First, analyses were conducted by our routine procedure, global normalization, in which each signal intensity was divided by the mean of each chip and multiplied by an arbitrary number to adjust the mean of each to the same value. In order to check the efficacy of the normalization procedure, the values of β-actin and GAPDH in each sample were divided by the mean value of the total 12 samples (Table 1). Expressed by this number, the values of β-actin varied between 0.91 - 0.99 in papilla, 0.98 - 1.12 in medulla, 0.97 - 1.14 in cortex, and 0.94 - 1.04 in the whole slice, resulting in an overall range of 0.91 - 1.14 (25% variation). The expression of GAPDH varied 0.76 - 0.85 in papilla, 1.01 - 1.05 in medulla, 1.11 - 1.19 in cortex, and 1.02 - 1.04 in the whole slice, resulting in an overall range of 0.76 - 1.19 (50% variation). Although they are relatively close to 1 (the mean value was 0.94, 1.02, and 1.03 for β-actin and 0.81, 1.03 and 1.16 for GAPDH in papilla, medulla, and cortex, respectively), the differences seemed to be too large to be ignored.

Using the data analyzed with global normalization, Pearson's correlation was calculated for each pair of the samples and is shown in Table 2A. The correlation coefficients were quite high among 3 samples from the same region, i.e., all were larger than 0.985. The correlation between papilla and others were lower than that between medulla and cortex, i.e., 0.821 - 0.860 between papilla and medulla, 0.741 - 0.789 between papilla and cortex, whereas it was 0.936 - 0.955 between medulla and cortex. The correlation coefficients between each of the three regions and the whole slice were in this order: cortex (0.981 - 0.987) > medulla (0.954 - 0971) > papilla (0.770 - 0.814), suggesting that gene expression in the whole slice preferentially represents that in cortex but it does not well represent that in papilla.

To try to identify genes with differential expression in the three regions, we first used a parameter of GeneChip data, detection call (present, marginal, and absent). Probe sets with present call in all samples in a region but all absent in other regions were selected as region-specific genes (Fig. 2). Genes with present call

Table 1. Signal intensity of β-actin and GAPDH.

Value type	Gene Title	Papilla			Medulla			Cortex			Whole		
		No.1	No.2	No.3	No.1	No.2	No.3	No.1	No.2	No.3	No.1	No.2	No.3
Signal intensity	β-actin	19619	20290	18700	20158	22911	20379	19881	23365	20759	19277	19278	21390
	GAPDH	17008	16029	15284	20169	21086	20291	22338	23834	23006	20765	20430	20458
Signal intensity	β-actin	0.95	0.98	0.90	0.98	1.11	0.99	0.96	1.13	1.00	0.93	0.93	1.03
Mean of signal intensity	GAPDH	0.85	0.81	0.77	1.01	1.06	1.02	1.12	1.20	1.16	1.04	1.03	1.03

Expression of β-actin and GAPDH in the three portions of kidney slice, papilla, medulla, and cortex, from three different rats (No. 1 - 3) as well as in the whole slice of three different rats (No. 4 - 6). Signal intensity of each gene was divided by the mean of all probes in the chip multiplied by 500 (global mean normalization, upper columns), after which each value was divided by the mean of these 12 values (per gene normalization).

in all samples of papilla but absent in all of medulla and cortex were 448, and only 27 (6%) were all present in the whole slice. Genes with present call in all samples of medulla but absent in others were quite rare, i.e., 18 probe sets, of which 2 (11%) had present call in all of the whole slices. Cortex-specific probes were found to be 44, and 34 (77%) were present in all of the samples of the whole slice. The relatively small number in the latter two portions indicates that most of the genes are common between medulla and cortex, and the gene expression in papilla is unique. These results suggest again that the region specific genes (in other than cortex) are difficult to detect by analysis of the whole slice.

The above results clearly indicate that the population of genes expressed in each region is quite different. Theoretically, absolute values of expression should be used when an accurate comparison is made between regions with different total mRNA contents. In order to further elucidate this point, the "percellome procedure" was employed to compare with global normalization.

The mean of copy numbers (or the values directly related to copy numbers) of β-actin was calculated to be 234, 291, 341, and 309 in papilla, medulla, cortex and the whole slice, respectively, i.e., the ratio in papilla, medulla, and cortex (whole slice = 1) was 0.76, 0.94 and 1.10, respectively. The mean of copy numbers of GAPDH was calculated to be 208, 298, 369 and 343, in papilla, medulla, cortex and the whole slice, respectively, i.e., the ratio in papilla, medulla, cortex (whole slice = 1) was 0.61, 0.87 and 1.08, respectively. These

Table 2. Pearson's correlation coefficient between samples.

A		Papilla			Medulla			Cortex			Whole		
		No1	No2	No3	No1	No2	No3	No1	No2	No3	No4	No5	No6
Papilla	No1	1	0.989	0.986	0.847	0.843	0.837	0.765	0.758	0.761	0.814	0.811	0.812
	No2		1	0.985	0.853	0.853	0.846	0.778	0.773	0.775	0.827	0.825	0.825
	No3			1	0.815	0.812	0.811	0.738	0.73	0.735	0.789	0.785	0.786
Medulla	No1				1	0.994	0.991	0.947	0.933	0.937	0.958	0.967	0.956
	No2					1	0.991	0.943	0.935	0.938	0.957	0.968	0.955
	No3						1	0.953	0.943	0.953	0.964	0.972	0.962
Cortex	No1							1	0.991	0.992	0.986	0.983	0.986
	No2								1	0.991	0.983	0.979	0.984
	No3									1	0.984	0.98	0.985
Whole	No4										1	0.996	0.994
	No5											1	0.992
	No6												1

B		Papilla			Medulla			Cortex			Whole		
		No1	No2	No3	No1	No2	No3	No1	No2	No3	No4	No5	No6
Papilla	No1	1	0.989	0.985	0.837	0.833	0.826	0.755	0.755	0.752	0.801	0.797	0.801
	No2		1	0.982	0.843	0.844	0.834	0.768	0.769	0.764	0.813	0.81	0.814
	No3			1	0.801	0.798	0.795	0.725	0.723	0.724	0.771	0.766	0.77
Medulla	No1				1	0.994	0.991	0.946	0.934	0.937	0.957	0.967	0.955
	No2					1	0.991	0.942	0.936	0.937	0.956	0.967	0.954
	No3						1	0.953	0.945	0.953	0.963	0.971	0.961
Cortex	No1							1	0.992	0.992	0.987	0.984	0.986
	No2								1	0.992	0.986	0.982	0.986
	No3									1	0.985	0.981	0.985
Whole	No4										1	0.996	0.994
	No5											1	0.992
	No6												1

0.90 –
0.85 –
0.80 –
0.75 –
– 0.75

A: Calculated on the data of global normalization.
B: Calculated on the data of percellome.

values clearly differ from those by global normalization, namely, the expression values in papilla were apparently overestimated by global normalization. The correlation coefficients calculated from the values normalized by percellome (Table 2B) were almost identical to that in Table 2A except between papilla and others, which showed a relatively large decrease in value. These results again indicated that global normalization was problematic, especially for papilla among the portions, most possibly because of the low amount of mRNA production in that region, compared with others.

After normalization either by global mean or percellome, the genes with absent call in all the samples were discarded and analyzed by ANOVA ($p<0.01$) in order to extract probe sets showing different expression in any region(s). The numbers of extracted probe sets were 12,322 for percellome and 8,161 for global normalization. Fig. 3 shows the results of K-means clustering (Euclidean, 10 clusters) of the expression values converted into z-scores in order to see the trend of expression in each region.

By percellome normalization (Fig. 3A), clusters of probe sets with characteristic region-dependent expression were efficiently extracted. It was also obvious from the figure that there was only one cluster containing only 293 probe sets that showed specifically high expression in papilla, and the other probe sets showed the lowest value in papilla compared to any other clusters. This indicates that most of the probe sets showed the lowest expression in papilla and the highest ones were exceptional. On the other hand, the clusters of global normalization (Fig. 3B) showed various, inconsistent patterns. Contrasting with the case of percellome normalization, there were many clusters in which gene expression was highest in papilla, or where papilla was equivalent to other region(s).

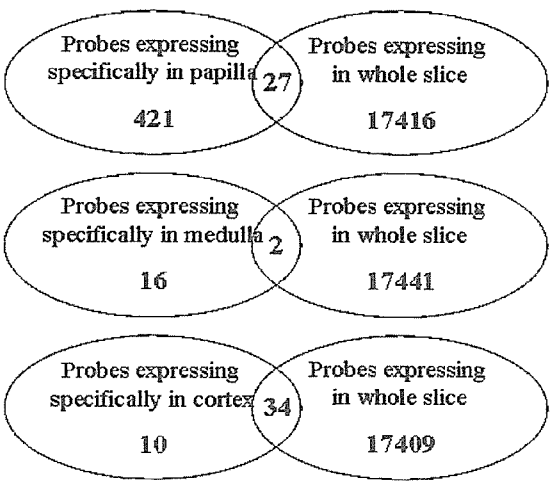

Fig. 2. Venn diagram of region-specific genes extracted by flags (present, absent and marginal call). The probes having "present call" in all samples of papilla and "absent call" in all samples of medulla and cortex were considered to be papilla-specific. The medulla- and cortex-specific probes were also extracted in the same manner and examined whether they were absent in the whole slice.

An obvious contradiction was noted between the two normalizations as described above, so further comparison was made. After the elimination of the probe sets that had absent call in all samples, the probe sets were classified into categories where the values showed maximum or minimum. Fig. 4 shows their counts in papilla, medulla, cortex, and whole slice for each normalization method. In the case of percellome normalization (A), the numbers of probe sets showing a maximal value were dominantly found in cortex, while the most of those showing a minimum were in papilla. On the other hand, in the case of global normalization (B), many of the probe sets showing their maximum were in papilla, while the numbers of probe sets with minimal expression were distributed evenly among the samples. It is noteworthy that very many (>3,000) probe sets showed minimal expression in the whole slice. However, this is theoretically impossible because the whole slice contains all the other 3 portions. Therefore, it should be concluded that the extraction of the genes with region-specific expression based on global normalization gives an error, and thus percellome normalization should be used in this case.

Based on the above results, region-specific genes in kidney were extracted as follows. After selection by ANOVA ($p<0.01$) for the data of percellome normalization, genes were categorized by the position at which they showed the larger expression value and then aligned in the order of their ratio to the minimum, for papilla (Table 3), medulla (Table 4) and cortex (Table 5). As is obvious from Figs. 3 and 4, the production of mRNA per cell was considered to be in the order of cortex>medulla>papilla, and the numbers of region-specific probe sets were also in this order. For simplicity, probe sets without any annotation were eliminated, and the ones with the ratio of >3 for papilla, >10 for medulla, and >30 for cortex, are presented in the tables.

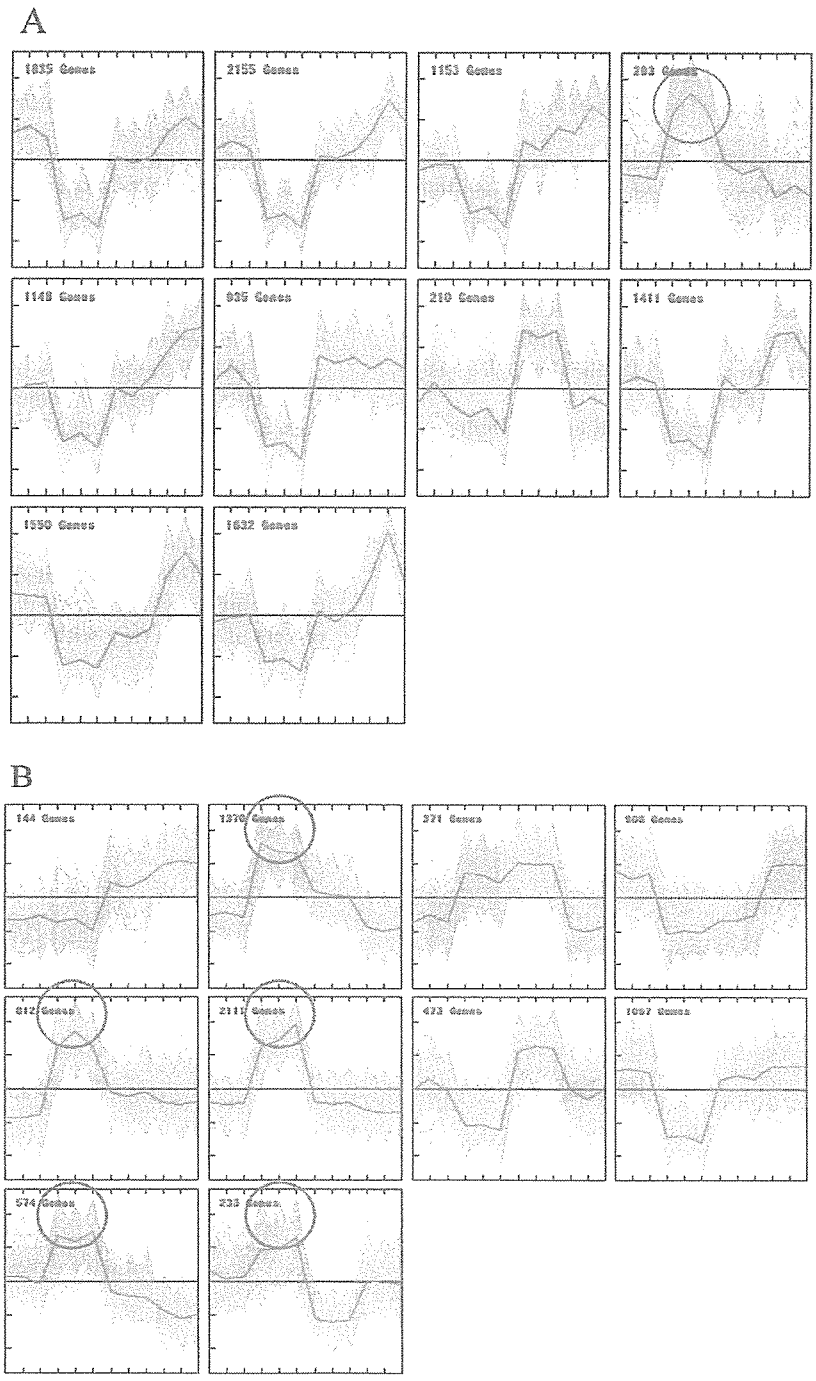

Fig. 3. K-means clustering of genes expressed in papilla, medulla, cortex, and whole slice of kidney. Data were processed by percellome normalization (A) or global mean normalization (B), and then converted into z-scores. K-means clustering (Euclidean, 10 clusters) was performed with MeV version 3.1 (The Institute for Genomic Research, Rockville, MD, USA). In each cluster, individual samples are aligned from left to right: whole slice (3), papilla (3), medulla (3), and cortex (3). Red lines indicatethe mean of the probes within each cluster. Orange circles indicate where papilla showed specifically high expression values.

In all these three tables, the higher rank is generally occupied by the genes related to channels, transporters and metabolic enzymes, suggesting that the gene lists are meaningful for analysis of specific renal functions.

In most of the papilla-enriched genes (Table 3), the ratio of papilla/cortex is larger than that of papilla/medulla, since the composition of papilla is closer to medulla than to cortex. The exceptional genes (highest in papilla and lowest in medulla) are shaded in the table. The outstanding feature of this table is that heat shock proteins and cytoskeleton/extracellular matrix proteins are present, in addition to the channel/transporters and metabolic enzymes.

In most of the medulla-enriched genes (Table 4), the ratio of medulla/cortex is less than 2, suggesting that their expression is relatively similar between these two portions. The genes with ratio of >3 are shaded in the table, but they are only 3 sets, indicating that medulla-specific genes are rare. The higher rank of the list in Table 4 is also occupied by channel/transporters and metabolic enzymes, and cytoskeletal proteins are scarce. A unique feature of medulla is the existence of 4 probe sets for prolactin receptor. This might occur simply because the quality of these multiple probes for one prolactin receptor is uniformly high.

Table 5 shows genes that showed the highest value in the cortex. It is noteworthy that many genes show more than 3 fold (shaded in the table) for the cortex/medulla ratio, indicating that there are many cortex-specific genes. The higher rank of this table is also occupied by channel/transporters and metabolic enzymes, but the numbers of metabolic enzymes are more prominent than in medulla.

Table 6 summarizes the genes categorized as channel/transporters, metabolic enzymes, cytoskeletons, and others for each portion.

DISCUSSION

The kidney is composed of various types of cells, and each portion (papilla, medulla, and cortex) has specific functions with wide variety, and the adverse effects of drugs vary with each portion. For example,

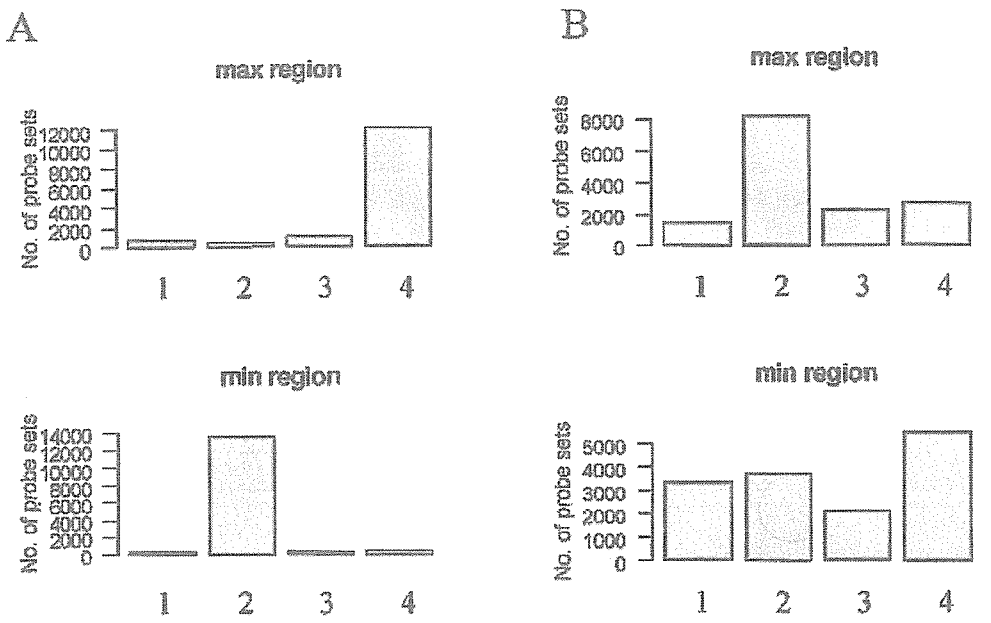

Fig. 4. The numbers of probe sets where their expression was maximal or minimal in whole slice, papilla, medulla, or cortex of kidney. After normalization by percellome (A) or global mean (B), probes with absent call in all samples were eliminated, and the numbers of probe sets with maximal (upper panels) or minimal (lower panels) were counted for each region, i.e., whole slice (1), papilla (2), medulla (3), and cortex (4).

Table 3. A list of probe sets specifically expressed in papilla of kidney.

Probe sets	papilla/ cortex	papilla/ medulla	medulla/ cortex	GENE_SYMBOL	GENE_NAME	channel transporter	Metabolic enzymes	cytoskeleton /extracellular matrix
1368259_at	32.0	12.7	2.5	Ptgs1	prostaglandin-endoperoxide synthase 1			
1389067_at	29.5	10.7	2.8	Slco4a1	solute carrier organic anion transporter family, member 4a1			
1372190_at	23.8	8.1	2.9	Aqp4	Aquaporin 4			
1394200_at	22.9	4.9	4.7	Hspa2	heat shock protein 2			
1387092_at	17.5	5.4	3.2	Fxyd4	FXYD domain-containing ion transport regulator 4			
1367847_at	17.4	5.4	3.2	Nupr1	nuclear protein 1			
1388460_at	16.8	5.6	3.0	Capg_predicted	capping protein (actin filament), gelsolin-like (predicted)			
1383469_at	7.2	14.6	0.5	Aldh1a3	Aldehyde dehydrogenase family 1, subfamily A3			
1376711_at	13.3	7.1	1.9	Cldn11	claudin 11			
1383319_at	13.2	2.5	5.3	Slc4a11_predicted	solute carrier family 4, sodium bicarbonate transporter-like, member 11 (predicted)			
1367734_at	13.1	7.9	1.7	Akr1b4	aldo-keto reductase family 1, member B4 (aldose reductase)			
1368765_at	10.7	2.5	4.2	Clcnk1	chloride channel K1			
1370229_at	10.5	1.9	5.4	Ndr4	N-myc downstream regulated 4			
1369841_at	10.3	4.2	2.4	Hspa2	heat shock protein 2			
1382303_at	3.8	8.8	0.4	RGD:1303187	phosphatase and actin regulator 1			
1378690_at	7.6	3.9	2.0	Ly6a_predicted	lymphocyte antigen 6 complex, locus A (predicted)			
1367661_at	6.8	3.7	1.8	S100a6	S100 calcium binding protein A6 (calcyclin)			
1374207_at	6.6	2.5	2.6	Agpt2	angiopoietin 2			
1369113_at	6.1	3.9	1.6	Grem1	gremlin 1 homolog, cysteine knot superfamily (Xenopus laevis)			
1368858_at	5.9	2.1	2.8	Ugt8	UDP-glucuronosyltransferase 8			
1368247_at	5.4	3.7	1.5	Hspa1a /// Hspa1b	heat shock 70kD protein 1A /// heat shock 70kD protein 1B			
1370334_at	3.2	5.4	0.6	Plekhb1	evectin-1			
1367650_at	5.1	3.1	1.6	Lcn7	lipocalin 7			
1374861_at	5.1	2.1	2.4	Tle2_predicted	transducin-like enhancer of split 2, homolog of Drosophila E(spl) (predicted)			
1387100_at	4.1	5.1	0.8	Aqp3	aquaporin 3			
1369949_at	5.0	3.6	1.4	Lu	Lutheran blood group (Auberger b antigen included)			
1369263_at	5.0	2.4	2.0	Wnt5a	wingless-type MMTV integration site 5A			
1370312_at	4.9	1.5	3.4	Spon1	spondin 1			
1388459_at	4.7	2.9	1.6	Col18a1	collagen, type XVIII, alpha 1			
1388456_at	4.3	3.0	1.4	S100a1	S100 calcium binding protein A1			
1393209_at	3.6	4.3	0.8	bsnd	Bartter syndrome, infantile, with sensorineural deafness (Barttin)			
1373733_at	4.3	2.8	1.5	Bok	Bcl-2-related ovarian killer protein			
1388547_at	4.2	2.5	1.7	Cldn4_predicted	claudin 4 (predicted)			

Table 3. Continued.

Probe sets	papilla/ cortex	papilla/ medulla	medulla/ cortex	GENE_SYMBOL	GENE_NAME	channel transporter	Metabolic enzymes	cytoskeleton /extracellular matrix
1396152_s_at	4.1	2.4	1.7	Igfbp5	insulin-like growth factor binding protein 5			
1367812_at	4.0	3.3	1.2	Spnb3	beta-spectrin 3			
1367577_at	3.4	3.9	0.9	Hspb1	heat shock 27kDa protein 1			
1372755_at	3.9	2.5	1.6	Mal2	mal, T-cell differentiation protein 2			
1370834_at	3.8	1.8	2.2	Hs3st1	heparan sulfate (glucosamine) 3-O-sulfotransferase 1			
1388155_at	3.8	3.3	1.2	Krt1-18	keratin complex 1, acidic, gene 18			
1372299_at	3.7	2.3	1.6	Cdkn1c	cyclin-dependent kinase inhibitor 1C (P57)			
1387886_at	3.6	2.7	1.3	Prelp	proline arginine-rich end leucine-rich repeat protein			
1368527_at	1.7	3.6	0.5	Ptgs2	prostaglandin-endoperoxide synthase 2			
1388102_at	1.9	3.5	0.5	Ltb4dh	leukotriene B4 12-hydroxydehydrogenase			
1370048_at	3.4	2.8	1.2	Edg2	endothelial differentiation, lysophosphatidic acid G-protein-coupled receptor, 2			
1371004_at	3.4	1.7	2.0	Sort1	sortilin 1			
1397830_at	3.4	2.3	1.5	Igfbp5	Insulin-like growth factor binding protein 5			
1369953_a_at	3.3	1.5	2.2	Cd24	CD24 antigen			
1367912_at	3.2	2.3	1.4	Ltbp1	latent transforming growth factor beta binding protein 1			
1387566_at	3.2	1.6	2.0	Pla2g4a	phospholipase A2, group IVA (cytosolic, calcium-dependent)			
1370912_at	3.2	2.3	1.4	Hspa1b	heat shock 70kD protein 1B			
1398318_at	3.2	2.1	1.5	Muc1	mucin 1, transmembrane			
1371625_at	3.1	2.8	1.1	Pygb	brain glycogen phosphorylase			
1370026_at	3.1	1.1	2.8	Cryab	crystallin, alpha B			
1393048_at	3.1	1.1	2.8	Adra2a	Adrenergic receptor, alpha 2a			
1388143_at	3.1	2.4	1.3	Col18a1	collagen, type XVIII, alpha 1			
1393958_at	3.1	2.1	1.5	Arhgap4	Rho GTPase activating protein 4			
1369084_a_at	3.1	2.8	1.1	Bok	Bcl-2-related ovarian killer protein			
1371499_at	3.0	1.8	1.7	Cd9	CD9 antigen			
1391830_at	3.0	1.9	1.6	Cpne8_predicted	copine VIII (predicted)			
1368342_at	3.0	1.9	1.6	Ampd3	adenosine monophosphate deaminase 3			
1384192_at	3.0	2.1	1.4	Chst1_predicted	carbohydrate (keratan sulfate Gal-6) sulfotransferase 1 (predicted)			
1398431_at	1.2	3.0	0.4	Car8_predicted	carbonic anhydrase 8 (predicted)			
1375170_at	3.0	1.6	1.9	S100a11_predicted	S100 calcium binding protein A11 (calizzarin) (predicted)			
1367759_at	3.0	1.2	2.5	H1f0	H1 histone family, member 0			
1387040_at	3.0	1.6	1.8	Mal	myelin and lymphocyte protein			

After selection by ANOVA ($p<0.01$) for the data of percellome normalization, genes maximally expressed in papilla were selected. The genes were aligned in the order of the ratio to the lower expression value, either in medulla or in cortex. As the genes listed here are expressed higher in medulla than cortex, in general, exceptional cases (ratio<0.6) are shaded in the medulla/cortex column. The genes categorized to "channel/transporters", "metabolic enzymes", or "cytoskeleton/extracellular matrix" are also shaded. Proteases or enzymes involving signal transduction are not included in the category of "metabolic enzymes". For simplicity, genes with less than 3-fold specificity are omitted.

Table 4. A list of probe sets specifically expressed in medulla of kidney.

Probe sets	medulla/ papilla	cortex/ papilla	medulla/ cortex	GENE_SYMBOL	GENE_NAME	channel transporter	Metabolic enzymes	cytoskeleton /extracellular matrix
1370377_at	204.8	124.5	1.6	Cyp2d9 /// Cyp2d10	cytochrome P450, family 2, subfamily d, polypeptide 9 /// cytochrome P450, family 2, subfamily d, polypeptide 10			
1387567_at	184.9	119.7	1.5	Slc21a1 /// LOC497799	solute carrier family 21, member 1 /// hypothetical gene supported by NM_017111			
1369401_at	153.0	69.6	2.2	Slc21a13	solute carrier family 21, member 13			
1387328_at	149.6	100.5	1.5	Cyp2c	Cytochrome P450, subfamily IIC (mephenytoin 4-hydroxylase)			
1368288_at	147.9	90.7	1.6	Gc	group specific component			
1368498_a_at	147.3	102.7	1.4	RGD:621387	kidney specific organic anion transporter			
1386454_at	133.0	46.7	2.8	Slc23a3_predicted	solute carrier family 23 (nucleobase transporters), member 3 (predicted)			
1370789_a_at	132.6	91.8	1.4	Prlr	prolactin receptor			
1387987_at	120.1	43.9	2.7	Slc22a19	solute carrier family 22 (organic anion transporter), member 19			
1390569_at	117.4	74.7	1.6	RGD:1359493	similar to carnosinase 1			
1369450_at	114.9	92.3	1.2	UST5r	integral membrane transport protein UST5r			
1369493_at	89.1	62.1	1.4	Prlr	prolactin receptor			
1368575_at	88.9	70.0	1.3	Slc6a18	solute carrier family 6 (neurotransmitter transporter), member 18			
1370824_at	88.2	60.3	1.5	Slc38a3	solute carrier family 38, member 3			
1387382_at	88.0	42.0	2.1	Hnmt	histamine N-methyltransferase			
1387303_at	83.1	59.2	1.4	Slc22a2	solute carrier family 22 (organic cation transporter), member 2			
1378247_at	81.5	41.3	2.0	Eaf2	ELL associated factor 2			
1373990_at	78.5	24.0	3.3	Slc7a12_predicted /// LOC361914	solute carrier family 7 (cationic amino acid transporter, y+ system), member 12 (predicted) /// similar to solute carrier family 7 (cationic amino acid transporter, y+ system), member 12			
1389756_at	78.0	57.9	1.3	Melk_predicted	maternal embryonic leucine zipper kinase (predicted)			
1384775_s_at	74.6	51.7	1.4	Tmprss8	transmembrane protease, serine 8 (intestinal)			
1370384_a_at	73.9	60.3	1.2	Prlr	prolactin receptor			
1368208_at	72.9	60.3	1.2	Cml1	camello-like 1			
1376944_at	72.5	68.6	1.1	Prlr	Prolactin receptor			
1385132_at	69.0	32.5	2.1	Mybl1_predicted	myeloblastosis oncogene-like 1 (predicted)			
1368651_at	66.4	49.0	1.4	Pklr	pyruvate kinase, liver and RBC			
1368304_at	65.8	57.1	1.2	Fmo3	Flavin containing monooxygenase 3			
1397205_at	54.9	42.8	1.3	Dhrs7_predicted /// LOC500672	dehydrogenase/reductase (SDR family) member 7 (predicted) /// similar to Down-regulated in nephrectomized rat kidney #3			